J Mater Sci (2007) 42:7004–7015
DOI 10.1007/s10853-006-1108-2

A fatigue-to-creep correlation in air for application to environmental stress cracking of polyethylene

Ravi Ayyer · Anne Hiltner · Eric Baer

Received: 17 July 2006 / Accepted: 3 October 2006 / Published online: 30 April 2007

Abstract The present study was undertaken to determine whether the correlation between fatigue and creep established for polyethylene in air could be extended to environmental liquids. Fatigue and creep tests under various conditions of stress, *R*-ratio (defined as the ratio of minimum to maximum load in the fatigue loading cycle), and frequency were performed in air and in Igepal solutions. The load–displacement curves indicated that stepwise fatigue crack growth in air was preserved in Igepal solutions at 50 °C, the temperature specified for the ASTM standard. In air, systematically decreasing the dynamic component of fatigue loading by increasing the *R*-ratio to $R = 1$ (creep) steadily increased the lifetime. In contrast, the lifetime in Igepal was affected to a much smaller extent. The fatigue to creep correlation in air was previously established primarily for tests at 21 °C. Before testing the correlation in Igepal, it was necessary to establish the correlation in air at 50 °C. Microscopic methods were used to verify stepwise crack growth by the sequential formation and breakdown of a craze zone, and to confirm the fatigue to creep correlation. The crack growth rate under various loading conditions was related to the maximum stress and *R*-ratio by a power law relationship. Alternatively, a strain rate approach, which considered a creep contribution and a fatigue acceleration factor that depended only on strain rate, reliably correlated fatigue and creep in air at 50 °C under most loading conditions of stress, *R*-ratio and frequency. The exceptions were fatigue loading under conditions of $R = 0.1$ and frequency less than 1 Hz. It was speculated that compression and bending of highly extended craze fibrils were responsible for unexpectedly high crack speeds.

R. Ayyer · A. Hiltner (✉) · E. Baer
Department of Macromolecular Science, and Center for Applied Polymer Research, Case Western Reserve University, Cleveland, OH 44106, USA
e-mail: ahiltner@case.edu

Introduction

Short-term fatigue testing is one approach to predicting long-term creep performance of engineering plastics. To accurately predict long-term failure, the failure mechanism must be maintained in fatigue while the crack growth kinetics is substantially accelerated. Previous results demonstrated that the relationship between fatigue and creep in a high density polyethylene resin can be quantitatively examined by systematically decreasing the dynamic component of fatigue loading [1]. This was accomplished by increasing the *R*-ratio, defined as the ratio of minimum to maximum load in the fatigue test, toward unity (creep loading). A power law relationship of the form:

$$\frac{da}{dt} = B' K_{\mathrm{I,max}}^{m} (1 + R)^{n} \tag{1}$$

where *da/dt* is the crack speed, $K_{\mathrm{I,max}}$ is the maximum stress intensity factor in the fatigue cycle (in creep $K_{\mathrm{I,max}} = K_{\mathrm{I}}$), *m* and *B′* are material constants, and the power *n* describes the sensitivity to *R*-ratio in fatigue. Equation 1 reduces to the common forms of the Paris law with power *m* for creep or fatigue under constant *R*-ratio.

Alternatively, varying the dynamic component of fatigue loading can be achieved by decreasing the fatigue test frequency toward zero (creep) [2]. Equation 1 is formulated for fatigue tests at a frequency of 1 Hz and does not accommodate crack growth rates measured at other

frequencies. To include the rate dependency explicitly, the expression for crack growth rate considers a creep contribution that depends only on stress intensity factor parameters and a fatigue contribution that depends only on strain rate:

$$\frac{da}{dt} = B\left\langle K_I^m(t)\right\rangle_T \beta(\dot{\varepsilon}) \tag{2}$$

where $B\left\langle K_I^m(t)\right\rangle_T$ is the creep contribution to the crack growth rate and is obtained by averaging the known dependence of da/dt on K_I^m in creep over the period T of the loading curve, and β is a function that depends only on strain rate. This approach to predicting long-term creep failure from short-term fatigue tests as developed for high density polyethylene was successfully extended to a medium density polyethylene pipe material at 21 °C [3], and to various PVC resins [4, 5].

Slow crack growth in polyethylene and other polymers can be strongly affected by surface active liquids, a phenomenon known as environmental stress cracking (ESC). The standard ESC creep test (ASTM D 1693-95) specifies a temperature of 50 °C and a 10% solution of Igepal CO 630 as the environmental liquid. The observation that Igepal CO 630 accelerated creep fracture only at lower stresses and longer creep failure times led to the concept of an Igepal transition time [6, 7]. This was qualitatively ascribed to accelerated fibril breakdown due to plasticization of the crystalline regions [8]. Further creep experiments with various nonreacting, nonswelling liquids led to the suggestion that ESC activity depended on the viscosity and the spreading coefficient of the liquid [9]. Several other studies described the accelerating effect of Igepal CO 630 on creep crack growth in polyethylene [10–12].

There have been only a few efforts to study the effect of environmental liquids on fatigue crack growth, and these have involved primarily glassy polymers [13, 14]. There appears to be no information regarding the effect of Igepal solution on fatigue crack propagation in polyethylene.

The present study was undertaken to determine whether the correlation between fatigue and creep established for polyethylene in air could be extended to environmental liquids. The correlation was previously established primarily for tests at 21 °C. In accordance with the ASTM standard, the environmental tests should be performed at 50 °C. However, increasing temperature introduces possible annealing effects and changes in failure mechanism. It was necessary to confirm the mechanism of fatigue crack propagation in air at 50 °C and to verify the fatigue to creep correlation at that temperature. In addition, this paper describes some preliminary results on fatigue crack propagation and lifetime in Igepal solutions of different molecular weight. The results are compared with tests in air.

Experimental

MDPE pipe material

Specimens were cut directly from the medium density polyethylene gas-pipe (ρ = 0.933 g/cc) that was used in a previous study [3]. The geometry and orientation of the compact tension specimens were the same as described previously [3]. The specimen thickness was 13 mm, the length defined as the distance between the line connecting the centers of the pin holes and the unnotched outer edge was 26 mm, the height to length ratio was 1.2, and the notch length was 12.5 mm. Specimens were notched in two steps: the initial 10 mm cut was made with a band saw and the final 2.5 mm cut was made with a razor blade driven at a controlled speed of 1μm/s at ambient temperature. A fresh razor blade was used for each specimen. All dimensions met the requirements of ASTM D 5045-93. To minimize plane stress edge effects, V-shaped side grooves 1 mm in depth were cut into the specimen.

Fatigue and creep testing

Tests were carried out in air or in a 10 vol% aqueous solution of an Igepal CO nonionic surfactant from Rhodia, Inc. The chemical structure of the Igepal CO series is

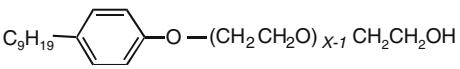

where x is the number of ethylene oxide units in the surfactant. The molecular weight, viscosity and surface tension varied depending upon the value of x. The kinematic viscosity was measured using Cannon Fenske type viscometer and calculated as $\eta = kt$ where η is the kinematic viscosity (cSt), k is an instrument constant equal to 0.008 (cSt/s) and t is the effluent time (s). The characteristics of the Igepal surfactants are given in Table 1.

Fatigue and creep tests were performed in an environmental chamber in air or in the presence of an Igepal solution. The specimens tested in air were mounted inside a constant temperature oven which could be controlled from –20 to 150 °C (±0.2°C). For environmental testing, specimens were immersed in a chamber containing the Igepal solution. The temperature was controlled using a circulating heat pump and could be regulated between –20 and 100 °C (±0.2°C). All tests were performed at 50 (±0.2)°C.

The mechanical fatigue units were capable of applying a stable and accurate (±0.5N) sinusoidal load in fatigue or constant load in creep tests. The load and crosshead displacement were recorded by computer. A manual zoom

Table 1 Characteristics of Igepal CO surfactants

Surfactant	x	Molecular weight (g/mol)	Surface tension ($\gamma_{\text{Igepal-air}}$ at CMC* (N/mm $\times$ 10^{-6})	Viscosity at 23 °C (cSt)
Igepal 997	~100	4620	50	15
Igepal 850	~25	1120	41	3
Igepal 630	~9	630	31	7

*From the technical datasheet of the supplier, Rhodia, Inc.

macrolens attached to a video camera was used to observe the crack tip. The camera was routed through a VCR and video monitor and, when the test was left unattended, the experiment was recorded onto a video cassette. The maximum and minimum crack tip opening displacement (CTOD), measured at the maximum and minimum stresses in the fatigue loading cycle, were taken from the video. The strain rate was then obtained as:

$$\dot{\varepsilon} = \left[\frac{\text{CTOD}_{\max} - \text{CTOD}_{\min}}{\text{CTOD}_{\min}}\right] 2f \tag{3}$$

where f is the frequency of the fatigue cycle.

The R-ratio (ratio of the minimum load to the maximum load in the fatigue cycle) was varied from 0.1 to 1.0 (creep) under constant $K_{\text{I,mean}}$ and constant $K_{\text{I,max}}$ conditions at frequency 1.0 Hz. Under constant mean stress, R was increased by decreasing the maximum stress and increasing the minimum stress. Under constant maximum stress, R was increased by increasing the minimum stress. Additional experiments in air were performed at various frequencies between 1.0 and 0.1 Hz.

Fracture surfaces were examined under the light microscope. Features were best resolved in bright field using normal incidence illumination.

Some specimens were loaded for a specific number of cycles, removed from the fatigue unit, and sectioned to obtain a side view of the craze damage zone ahead of the crack tip. The sections were coated with 9 nm of gold and examined in a JEOL JSM 840A scanning electron microscope. The accelerator voltage was 15 kV and the probe current was 6×10^{-11} amps to minimize radiation damage to the specimens. Sections were placed on a special SEM sample holder that held the crack tip open.

Other specimens were loaded for a specific time under $K_{\text{I,mean}} = 0.65$ MPa $\text{m}^{1/2}$ in creep or fatigue at $R = 0.1$, removed from the unit and sectioned as thin as possible (~0.1mm) to obtain the side view of the craze damage zone ahead of the crack tip. To resolve the yielded damage zone around the craze, sections were etched in a solution of 0.7 wt% $KMnO_4$ in 1:2 sulphuric acid and ortho-phosphoric acid (by volume) at ambient temperature. The images were obtained in the transmission mode of the light microscope.

Results and discussion

Effect of R-ratio on fatigue and creep crack growth in air and Igepal

The relationship between fatigue and creep was examined by systematically decreasing the dynamic component of fatigue loading. This was accomplished by varying the R-ratio, defined as the ratio of the minimum stress to the maximum stress in the fatigue loading cycle, so that R gradually approached unity (creep loading). The R-ratio was varied under conditions of constant K_{mean} and constant $K_{\max}$. Typical crosshead displacement curves for creep and fatigue tests at constant $K_{\text{I,mean}} = 0.65$ MPa $\text{m}^{1/2}$ are shown in Fig. 1. The curves in both air and Igepal at 50 °C revealed stepwise crack growth, which resulted from sequential formation and breakdown of a craze damage zone that formed ahead of the crack tip [15]. The plateau regions in Fig. 1 corresponded to periods of crack arrest, during which the damage zone was stable. The sharp increases in crosshead displacement corresponded to step jumps where the craze damage zone fractured and a new one began to form. Stepwise crack growth was confirmed by the presence of striations on the fracture surface. The exceptions were the displacement curves for fatigue at $R = 0.7$ and for creep in air, which did not exhibit the well-defined steps that characterized the other fatigue curves and the creep curves under other loading conditions. Additional fatigue and creep tests performed at constant $K_{\text{I,max}} = 1.00$ MPa $\text{m}^{1/2}$ all exhibited well-defined steps in the load–displacement curves.

The effect of R-ratio on lifetime under constant $K_{\text{I,mean}}$ and constant $K_{\text{I,max}}$ is shown in Fig. 2. In air, the lifetime steadily increased as R-ratio approached creep. As expected, the effect of R-ratio was larger under $K_{\text{I,mean}}$ loading than under $K_{\text{I,max}}$ loading. Under constant $K_{\text{I,mean}}$ loading, $K_{\text{I,max}}$ steadily decreased as R-ratio approached 1.0 (creep). The results in air at 50 °C closely followed the trends reported previously for high density polyethylene (HDPE) at 21 °C [1]. Similar experiments were not performed previously on MDPE at 21 °C because of the very long fracture times for $R > 0.4$ [3].

In Igepal 997, the fatigue acceleration effect was observed only at lower R-ratio. The overall lifetime in Igepal 997 was comparable to that in air for lower R-ratio (0.1–0.5). However for higher R-ratio (0.7 and creep), the lifetime in Igepal 997 only slightly increased under $K_{\text{I,mean}}$ loading and slightly decreased under $K_{\text{I,max}}$ loading. For creep, the lifetime in Igepal 997 was on the order of five times lower than in air, Table 2.

The lifetime in Igepal 850 and Igepal 630 was slightly longer than in air for $R = 0.1$. The crack tip strain rate was highest at $R = 0.1$. It was possible that heat generated at the

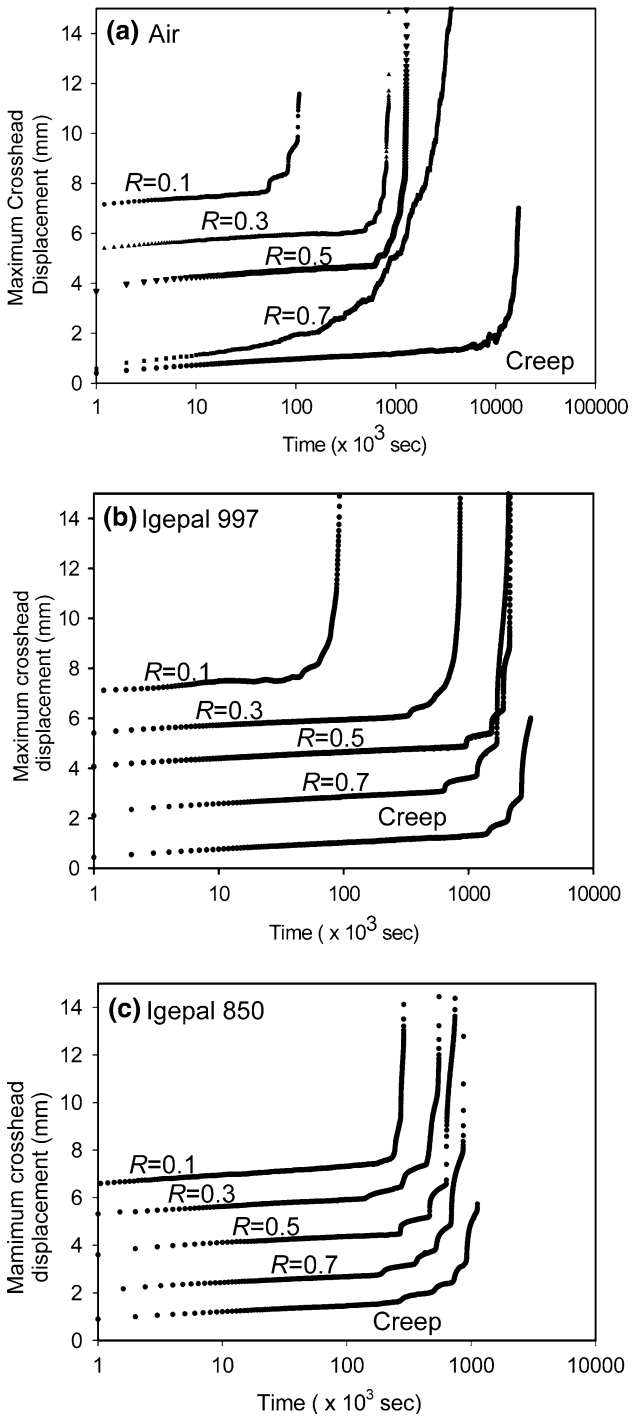

Fig. 1 Crosshead displacement during fatigue and creep tests of MDPE at 50 °C and $K_{I,mean}$ = 0.65 MPa $m^{1/2}$: (**a**) In air; (**b**) in Igepal 997; and (**c**) in Igepal 850. Curves are shifted vertically for clarity

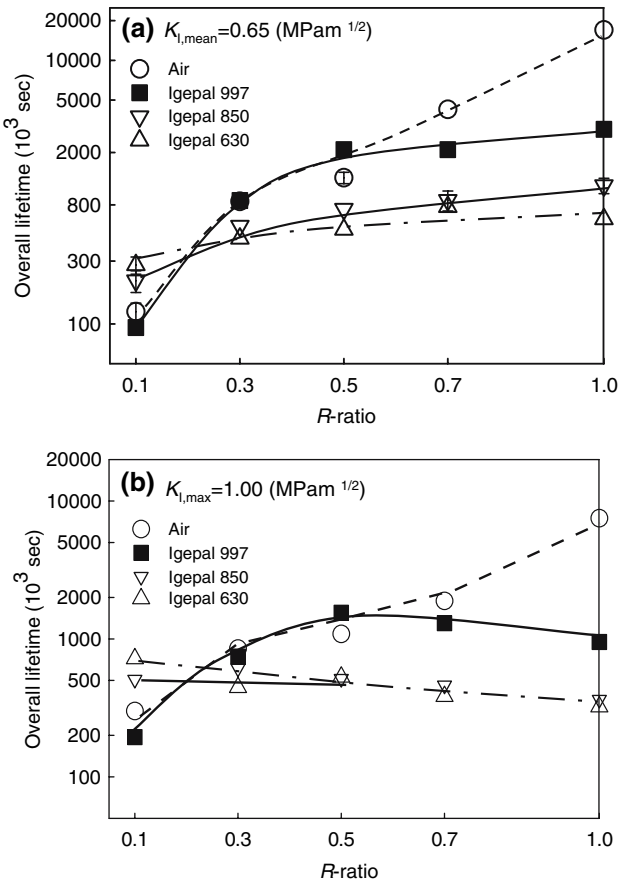

Fig. 2 Lifetimes at 50 °C in air and Igepals as a function of *R*-ratio: (**a**) Constant $K_{I,mean}$ and (**b**) constant $K_{I,max}$

crack tip was more effectively dissipated in the environmental liquid than in air. For R = 0.3, the lifetime in Igepal 850 and Igepal 630 was slightly lower than in air. The environmental effect became increasingly apparent at higher *R*-ratio (0.5 to creep), where the lifetime was substantially lower than in air. Overall, the lifetime in Igepal 850 and Igepal 630 was not very sensitive to *R*-ratio. With increasing *R*-ratio, the lifetime slightly increased under $K_{I,mean}$ loading and slightly decreased under $K_{I,max}$ loading.

The conservation of a stepwise crack propagation mechanism and the smooth increase in lifetime from fatigue to creep indicated that short-term fatigue testing could predict long-term fracture in air. Although fatigue in Igepal appeared to follow stepwise propagation, as in air, the fatigue acceleration effect was much weaker or nonexistent for Igepal 850 and Igepal 630. This suggested that Igepal affected the craze damage zone ahead of the crack tip and/or the failure mechanism of the craze fibrils.

As the basis for probing the environmental effect of Igepal, the relationship between fatigue and creep in air at 50 °C needed to be established. Although the fatigue to creep correlation for MDPE in air was previously demonstrated at 21 °C [3], it was necessary to confirm the result for the elevated temperature of the environmental tests, where decreasing yield stress reduced the range in $K_{I,max}$ for slow stepwise crack growth. The previously established testing protocol was followed.

Table 2 Results of fatigue and creep tests in different environments at 50 °C and frequency 1.0 Hz

R-ratio	$K_{I,mean}$ (MPa $m^{1/2}$)	$K_{I,max}$ (MPa $m^{1/2}$)	Overall lifetime (10^3 s)
Air			
0.1	0.645	1.170	124 ± 20
0.3	0.650	1.000	851 ± 100
0.5	0.652	0.869	1286 ± 120
0.7	0.650	0.765	4,990
1.0 (creep)	0.650	0.650	17,035
0.1	0.550	1.000	300
0.5	0.750	1.000	1,086
0.7	0.850	1.000	1,884
1.0 (creep)	1.000	1.000	7,500
Igepal 997			
0.1	0.645	1.170	94±10
0.3	0.650	1.000	863
0.5	0.652	0.869	2,174
0.7	0.650	0.765	2,150
1.0 (creep)	0.650	0.650	3,000
0.1	0.550	1.000	194
0.5	0.750	1.000	1,435
0.7	0.850	1.000	1,300
1.0 (creep)	1.000	1.000	1,850
Igepal 850			
0.1	0.645	1.170	220 ± 40
0.3	0.650	1.000	611
0.5	0.652	0.869	743
0.7	0.650	0.765	869 ± 150
1.0 (creep)	0.650	0.650	1,124 ± 150
0.1	0.550	1.000	507
0.5	0.750	1.000	515
0.7	0.850	1.000	461
1.0 (creep)	1.000	1.000	363
Igepal 630			
0.1	0.645	1.170	270 ± 42
0.3	0.650	1.000	445
0.5	0.652	0.869	519
0.7	0.650	0.765	774
1.0 (creep)	0.650	0.650	624
0.1	0.550	1.000	726
0.5	0.750	1.000	529
0.7	0.850	1.000	385
1.0 (creep)	1.000	1.000	322

Fracture surfaces in air

The fracture surfaces for selected tests at constant $K_{I,mean}$ loading and constant $K_{I,max}$ loading are shown in Fig. 3. For fatigue, periodic striations were observed on the fracture surfaces at each *R*-ratio. The number of striations on the fracture surface corresponded with the number of step jumps on the crosshead displacement curve for each test. For constant $K_{I,mean}$ = 0.65 MPa $m^{1/2}$, the step jump length, defined as the distance between the striations, was about the same for each *R*-ratio, Table 3. The exceptions were the fracture surfaces for R = 0.7 and for creep under constant K_I = 0.65 MPa $m^{1/2}$, which showed short, indistinct step jumps. For constant $K_{I,max}$ = 1.00 MPa $m^{1/2}$, all the fracture surfaces including creep exhibited well-defined striations. In this case, the step length increased with *R*-ratio from R = 0.1 to creep.

The correlation between the step jumps on the displacement curve and the formation and fracture of the craze damage zone was established by loading a specimen to a prescribed number of cycles at 50 °C, removing it from the fatigue unit, sectioning it through the damage zone, and viewing it in the light microscope in the reflection mode. The formation and fracture of the first craze zone for loading under $K_{I,mean}$ = 0.65 MPa $m^{1/2}$and R = 0.1 is shown in Fig. 4. The crack-tip craze zone reached about 90% of its final length within 20% of the first step lifetime, Fig. 4a. Subsidiary shear crazes emerged from the membrane at the crack tip at an angle of about 30° to the main craze. The craze zone intensified at 80% of the lifetime, Fig. 4b. The craze zone started to fracture at the step jump on the displacement curve, leaving a membrane at the crack tip, and a new zone started to form, Fig. 4c. At the end of the first step jump the membrane had ruptured and the second craze zone was well developed including a new set of shear crazes at the crack tip, Fig. 4d. The ruptured membrane produced the characteristic striation on the fracture surface. Correspondence between the step jump length in Fig. 3 and the length of the main craze in Fig. 4 confirmed that the crack jumped through the main craze.

Fatigue and creep experiments were conducted under a variety of loading conditions at 50 °C and all the results are compiled in Table 3. In previous experiments at other temperatures, $K_{I,mean}$ was found to control step jump length [3]. The first step length for tests at all *R*-ratios and frequency 1 Hz is plotted versus $K^2_{I,mean}$ in Fig. 5. Only results for R = 0.7 and creep under constant K_I = 0.65 MPa $m^{1/2}$, which showed short and indistinct step jumps, are omitted from the figure. The squared dependence is consistent with the Dugdale model prediction for the length l of the plastic zone at constant load

$$l = \frac{\pi}{8}\frac{K_I^2}{\sigma_y^2} \tag{4}$$

provided that $K_I = K_{I,mean}$. The yield stress in Eq. 4 is a viscoelastic parameter that depends on strain rate and temperature. From the fit to the Dugdale expression, the

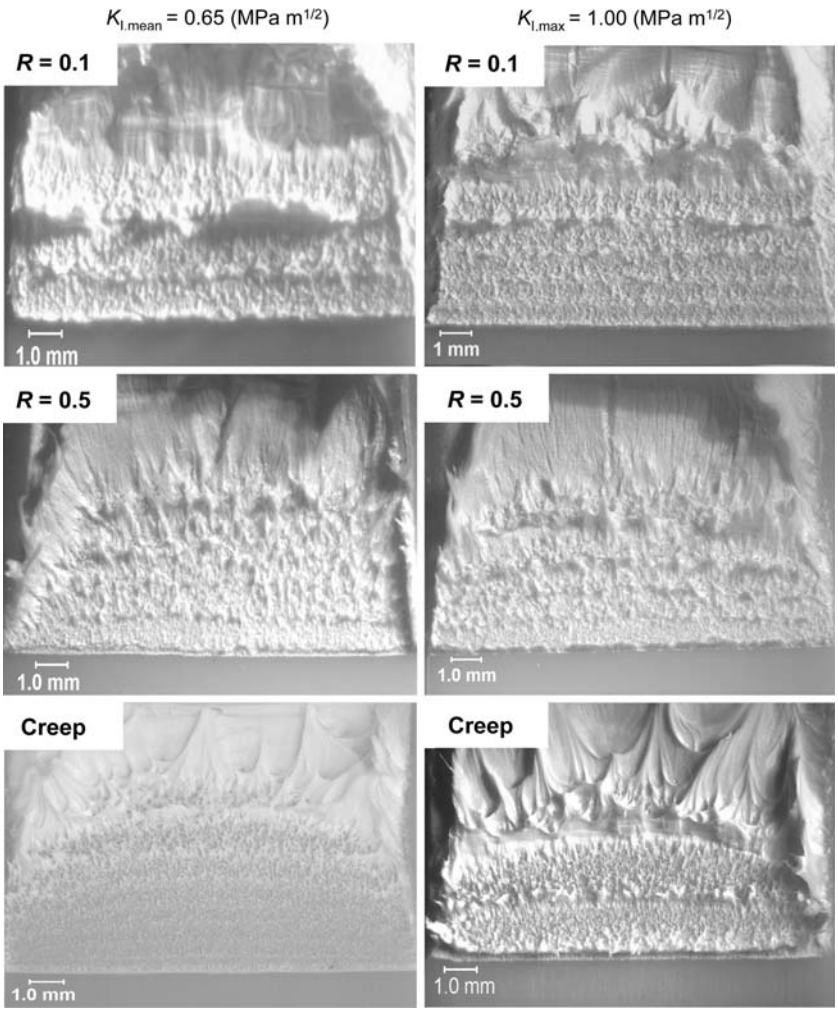

Fig. 3 Effect of R-ratio on the fracture surface of compact tension specimens tested at 50 °C in air at constant $K_{I,mean}$ and at constant $K_{I,max}$

extracted yield stress at 50 °C was 13.6 MPa, which agreed well with the measured yield stress of 13.2 MPa.

The origin of the uncharacteristically short, indistinct step jumps on the fracture surfaces of $R = 0.7$ and of creep at 50 °C and $K_{I,mean} = 0.65$ MPa m$^{1/2}$, and the absence of well-defined steps jumps on the displacement curve, was probed by examination of the crack tip damage zone. At Position 1 on the creep displacement curve in Fig. 6, a craze-like zone had formed at the crack tip which was much shorter than the craze zone in fatigue (compare with Fig. 4). The craze-like zone was not accompanied by shear crazes. At Position 2, the initial craze-like zone had broken and a new, short craze-like zone had formed. However there was no identifiable step on the displacement curve to indicate when the zone fractured. It appeared that the crack-tip damage zone was different under this $K_{I,mean}$ condition.

Thinner, etched fatigue ($R = 0.1$) and creep specimens are compared in the transmission light microscope in Fig. 7. The strong main craze with adjoining shear crazes of the $R = 0.1$ fatigue specimen was typical of the brittle failure mechanism in MDPE. However in creep, a small diffuse damage zone was evident at the crack tip in addition to the short craze-like zone. The yielded zone prevented formation of shear crazes and inhibited growth of the craze-like zone. A similar crack tip damage zone with a diffuse yielded region superimposed on an intense line zone was previously reported in polypropylene [16].

A change in the crack tip damage zone compromised the possibility for establishing a fatigue to creep correlation at 50 °C. However, creep tests performed at higher K_I of 0.87 and 1.00 MPa m$^{1/2}$ exhibited the typical features of stepwise fracture with large well-defined steps on the fracture surface (see Fig. 3). Results for these creep tests were used to establish the fatigue to creep correlation.

Kinetics of crack propagation

The crack growth rate (da/dt) for stepwise crack growth is calculated by dividing the step jump length by the lifetime of the step jump. For a given R-ratio, the dependence of crack growth rate on the stress intensity is expressed by the Paris relationship:

Table 3 Results of fatigue and creep tests in air at 50 °C

R-ratio	*f* (Hz)	$K_{I,mean}$ (MPa $m^{1/2}$)	$K_{I,max}$ (MPa $m^{1/2}$)	First step length (mm ± 0.1)	First step lifetime (× 10^3 s)	Overall lifetime (× 10^3 s)	Strain rate	$CTOD_{max}$(mm)	Δ CTOD (mm)
0.1	1.0	0.645	1.170	1.0	62 ± 9	124 ± 20	0.810	0.500	0.145
0.3	1.0	0.650	1.000	0.9	500 ± 80	851 ± 100	0.460	0.398	0.075
0.5	1.0	0.652	0.869	1.1	644 ± 85	1,286 ± 120	0.270	0.315	0.037
0.7	1.0	0.650	0.765	0.6	1,350	4,990	0.074	0.265	0.009
1.0 (creep)	–	0.650	0.650	0.5	–	17,035	–	0.242	–
1.0(creep)	–	0.869	0.869	1.3	5,720	9,993	–	0.257	–
0.1	1.0	0.550	1.000	0.6	90	300	0.740	0.435	0.118
0.5	1.0	0.750	1.000	1.1	563	1,086	0.320	0.344	0.048
0.7	1.0	0.850	1.000	1.3	905	1,884	0.110	0.297	0.015
1.0 (creep)	–	1.000	1.000	1.9	4,500	7,500	–	0.264	–
0.1	1.0	0.597	1.086	1.0	84	215	0.750	0.467	0.127
0.1	1.0	0.693	1.260	1.1	55	96	0.850	0.533	0.158
0.1	0.3	0.645	1.170	0.9	112	270	0.400	0.520	0.210
0.1	0.1	0.645	1.170	1.2	171	348	0.200	0.548	0.274
0.1	0.03	0.645	1.170	1.2	248	490	0.040	0.673	0.269
0.1	0.1	0.597	1.086	0.9	190	480	0.127	0.509	0.198
0.1	0.03	0.597	1.086	1.0	280	640	0.035	0.635	0.234
0.1	0.5	0.75	1.000	1.1	871	1,665	0.028	0.407	0.050
0.1	0.7	0.850	1.000	1.3	1,284	2,824	0.012	0.314	0.017

$$\frac{da}{dt} = A\Delta K_I^m \tag{5}$$

where ΔK_I is the difference between the maximum and minimum stress intensity factors in the fatigue cycle and A and m are material parameters. The value of m was previously determined to be independent of temperature and R-ratio, and equal to four for polyethylene [3, 17, 18]. The double logarithmic plot of da/dt vs. ΔK_I in Fig. 8 compares the data for various R-ratios at 50 °C. The data conformed to $m = 4$ and the parameter A increased with increasing R-ratio.

For constant frequency, only two of the loading parameters (R-ratio, ΔK_I $K_{I,max}$, $K_{I,min}$ and $K_{I,mean}$) can be varied independently. The effects of $K_{I,max}$ and $K_{I,mean}$ on crack growth rate at 50 °C were separated by varying R-ratio under conditions of constant $K_{I,max}$ or constant $K_{I,mean}$. The effect of $K_{I,mean}$ was obtained by constructing a double logarithmic plot of the first step crack growth rate vs. $K_{I,mean}$ for tests under constant $K_{I,max}$ = 1.00 MPa $m^{1/2}$ as shown in Fig. 9a. The regression line through the data indicated that the crack growth rate followed a $K_{I,mean}^{-6}$ dependence. Similarly, the effect of $K_{I,max}$ was obtained by constructing a double logarithmic plot of the first step crack growth rate vs. $K_{I,max}$ for tests under constant $K_{I,mean}$ = 0.65 MPa $m^{1/2}$, Fig. 9b. The results indicated a $K_{I,max}^{10}$ dependence of crack growth rate.

From the dependence of crack growth rate on $K_{I,max}$ and $K_{I,mean}$ an empirical power law relation was constructed to describe the crack growth rate at all R-ratios:

$$\frac{da}{dt} = BK_{I,max}^{10}K_{I,mean}^{-6} \tag{6}$$

In creep, $K_{I,max} = K_{I,mean} = K_I$ and Eq. 6 reduces to the Paris law for creep in polyethylene [3]:

$$\frac{da}{dt} = BK_I^4 \tag{7}$$

In order to facilitate the fatigue to creep correlation, Eq. 6 was reformulated using the definitions of $R = \frac{K_{I,min}}{K_{I,max}}$ and $K_{I,mean} = \frac{K_{I,max}+K_{I,min}}{2}$ to obtain:

$$\frac{da}{dt} = B'K_{I,max}^4(1+R)^{-6} \tag{8}$$

A more general form of Eq. 8 is expressed as Eq. 1. The power m in the term $K_{I,max}^m$ appears to be equal to 4 for all polyethylenes. The term $(1 + R)^n$ is a measure of the sensitivity of the resin to R-ratio in fatigue. The power n is characteristic of the specific resin, but comparison with previous results for the same MDPE resin at other temperatures indicates that n is independent of temperature [1, 3]. The parameter B' is a material constant specific to the MDPE resin and increases with increasing temperature.

In creep (R = 1.0), Eq. 1 reduces to:

$$\frac{da}{dt} = 2^n B'K_I^m \tag{9}$$

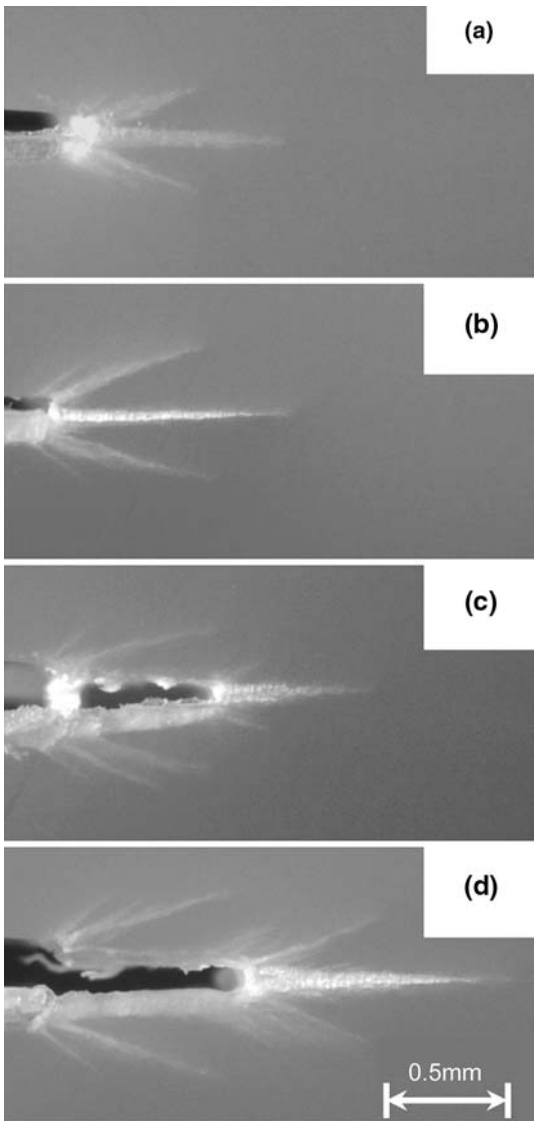

Fig. 4 Light micrographs of the crack tip damage zone showing the periodical formation and fracture of the craze during stepwise fatigue crack propagation at 50 °C: (**a**) 20,000 cycles; (**b**) 58,000 cycles; (**c**) 74,000 cycles; and (**d**) 97,000 cycles. The compact tension specimens were loaded under $K_{I,mean}$ = 0.65 MPa $m^{1/2}$ and R = 0.1

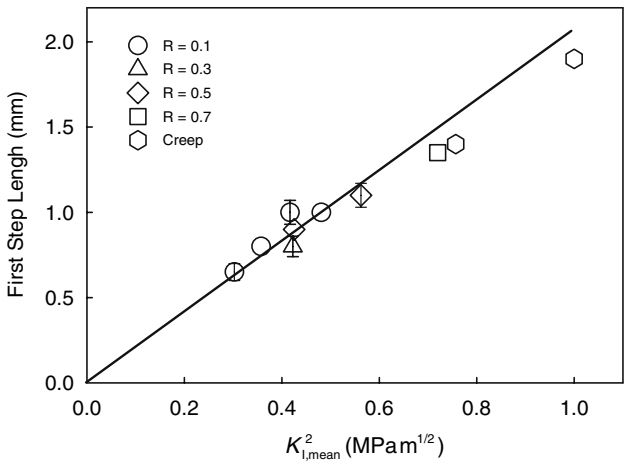

Fig. 5 Dependence of the first step length on the square of $K_{I,mean}$

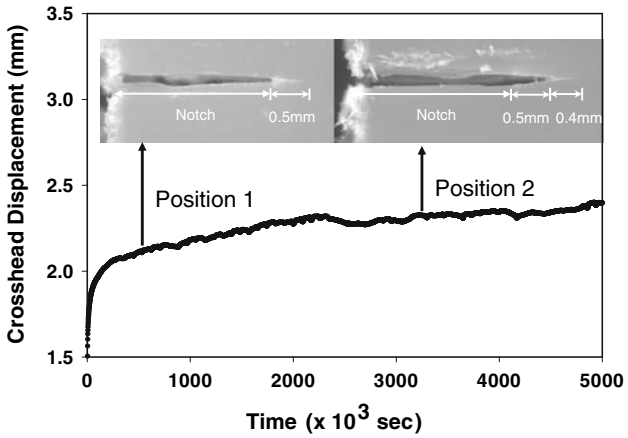

Fig. 6 The crosshead displacement curve for creep at K_I = 0.65 MPa $m^{1/2}$. The optical micrographs show the crack tip damage zone after the creep test was stopped at the positions indicated

with the requirement that the power m is the same in fatigue and creep. Then, $2^n B'$ is a measure of creep crack growth resistance, and the factor B in the Paris law for creep is obtained from B' as $B = 2^n B'$.

The fatigue and creep data are plotted according to Eq. 8 in Fig. 10. All the results for crack growth rate at 50 °C are described by a single regression line when plotted as a function of $K^4_{I,max}(1 + R)^{-6}$. The value of the parameter B' extracted from the fit is 1.7 mm m^2/s/MPa^4. Accordingly, the creep prefactor $B = (B'/2^6)$ at 50 °C is 0.026×10^{-5} (mm m^2/s/MPa^4). Considering the creep data only, the value of B obtained directly from the Paris law for creep is 0.036×10^{-5} (mm m^2/s/MPa^4). Given the long duration of the creep experiments, the two values are in good agreement. An Arrhenius plot of ln B' vs. 1/T for the same MDPE resin exhibited a change in slope at about 55 °C [3]. The B' value for 50 °C fit on the line for lower temperature behavior.

Strain rate effect

Equation 6 is formulated for fatigue tests at a frequency of 1 Hz and does not accommodate crack growth rates measured at other frequencies. To include the rate dependency explicitly, an alternative approach was developed for HDPE [2], and for MDPE [3], at 21 °C. The expression for crack growth rate considers a creep contribution that depends only on stress intensity factor parameters and a fatigue contribution that depends only on strain rate:

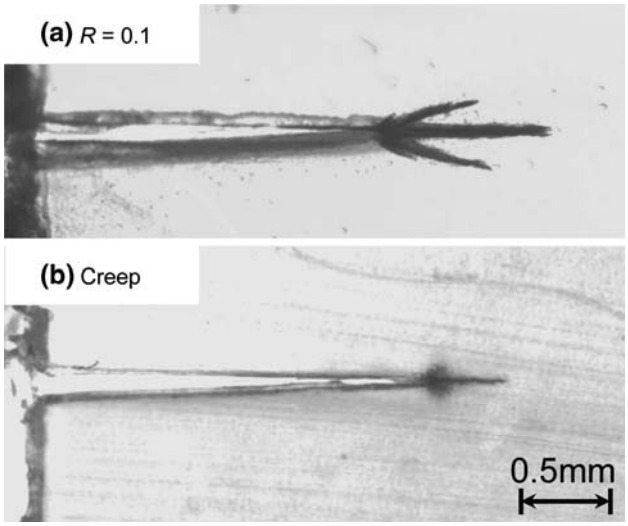

Fig. 7 Transmission light micrographs comparing the crack tip damage zone in fatigue and creep: (**a**) The fatigue specimen in Fig. 4b loaded at K_{Imean} = 0.65 MPa m$^{1/2}$ and R = 0.1; and (**b**) the creep specimen at Position 1 in Fig. 6 loaded at K_{I} = 0.65 MPa m$^{1/2}$

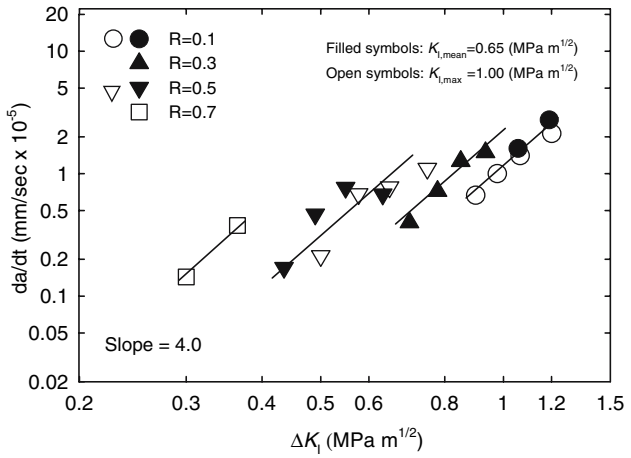

Fig. 8 Paris plots of crack growth rate vs. ΔK_{I} for fatigue at various R-ratios

$$\frac{da}{dt} = B\left\langle K_I^4(t)\right\rangle_T \beta(\dot{\varepsilon}) \tag{10}$$

where $B\left\langle K_I^4(t)\right\rangle_T$ is the creep contribution to the crack growth rate and is obtained by averaging the known dependence of da/dt on K_I^4 in creep over the period T of the sinusoidal loading curve:

$$\left(\frac{da}{dt}\right)_{\text{creep}} = B\left\langle K_{\text{I}}^4(t)\right\rangle_T = \frac{B}{T}\int_T K_{\text{I}}^4(t)dt \tag{11}$$

The parameter B was obtained from the experimental B'.

The term $\beta(\dot{\varepsilon})$ is the fatigue acceleration factor. In the case of HDPE and MDPE, $\beta(\dot{\varepsilon})$ is a linear function of strain rate [2, 3]:

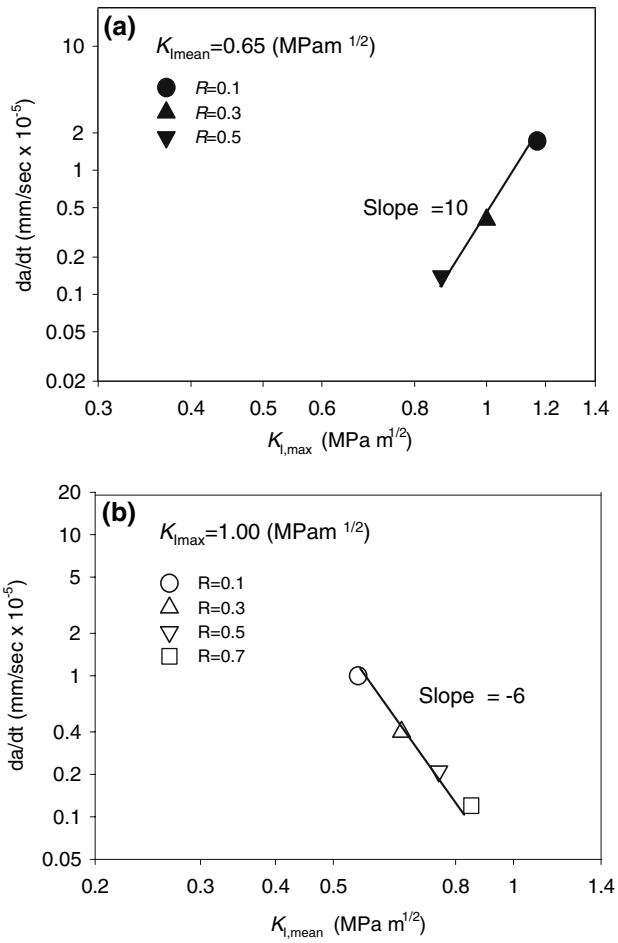

Fig. 9 Fits of fatigue crack growth rate to: (**a**) $K_{\text{I,max}}$; and (**b**) $K_{\text{I,mean}}$

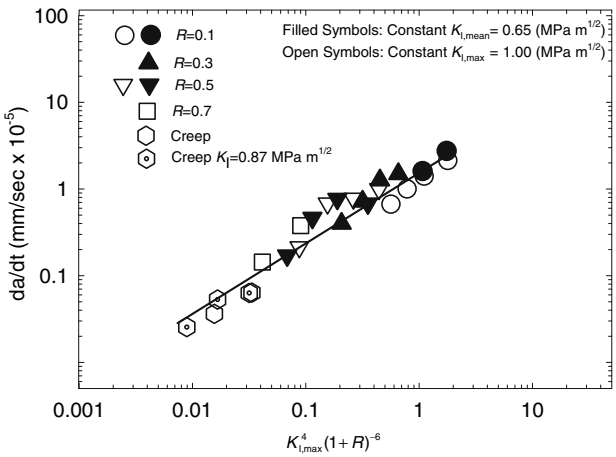

Fig. 10 Fit of all crack growth rate data to $K_{\text{I,max}}^4$ $(1 + R)^{-6}$ dependence

$$\beta(\dot{\varepsilon}) = (1 + C\dot{\varepsilon}) \tag{12}$$

The parameter C is a measure of the strain rate sensitivity in fatigue testing and depends on temperature.

Varying the R-ratio changes the strain rate of craze opening during the fatigue cycle. The relationship between strain rate at the crack tip, as measured from CTOD, and R-ratio is plotted as $(1-R)=\frac{\Delta K_I}{K_{I,max}}$ in Fig. 11 for all tests at frequency 1 Hz. The data were described by a power law regression as $\dot{\varepsilon}=0.95(1-R)^{2.0}$ for strain rate expressed in s^{-1}. For comparison, the power law regression was $\dot{\varepsilon}=0.65(1-R)^{3.2}$ for data obtained at 21 °C [3]. The higher strain rate for a given R-ratio reflects the larger crack opening displacement at 50 °C.

A larger variation in strain rate was obtained by decreasing the frequency of the fatigue cycle. Results for fatigue tests performed at various frequencies are included in Table 3. All the tests exhibited stepwise crack propagation. The first step length conformed to the Dugdale relationship as expressed in Eq. 4, except for tests at R = 0.1 and frequency 0.1 or 0.03 Hz. In these cases, the first step length was about 20% longer than anticipated.

The crack growth rate from the first step lifetime normalized to $B\langle K_I^4(t)\rangle_T$ is plotted against the experimentally determined strain rate for all the fatigue tests at varying R-ratio and varying frequency in Fig. 12. With some experimental scatter, most of the data could be considered to fall on a line that extrapolated to unity at zero strain rate. The exceptions were data obtained at R = 0.1 and frequency 0.1 or 0.03 Hz. Under these loading conditions, crack speed was considerably higher than expected based on Eq. 10.

The linear relationship that described most of the data in Fig. 12 confirmed the origin of fatigue acceleration in a strain rate effect. The same functional relationship between strain rate and crack speed at both 50 and 21 °C confirmed the correspondence in the stepwise mechanism of crack propagation. However, temperature affected the magnitude of the fatigue acceleration effect as represented by the parameter C in Eq. 12. A decrease in C from 260 s at 21 °C [3], to 120 s at 50 °C indicated that stepwise crack propagation became less strain rate sensitive as the temperature increased. Fatigue crack propagation in HDPE was even less strain rate sensitive, with C reported to be 19 s at 21 °C [2].

For creep, fibril fracture is ascribed to chain disentanglement through the processes of chain slippage and pullout [19–21]. For fatigue, the mechanism of fibril deterioration is still unknown. Correlation between fatigue and creep is the basis for speculation that disentanglement contributes significantly to fatigue failure. However, in a glassy polymer, fatigue was thought to accelerate the crack growth rate by enhancing the rate of chain scission in PVC. It is speculated that breakage also contributes to fatigue acceleration in polyethylene, especially when features of the molecular architecture such as branching make the chains resistant to pullout. It can be imagined that increasing temperature facilitates chain pullout more than chain breakage [4, 22]. As a result, slow crack growth in MDPE become less strain rate sensitive as reflected by a decrease in the parameter C. Nevertheless, even at 50 °C, MDPE has much higher strain rate sensitivity than HDPE at 21 °C.

Unexpectedly high crack speeds were observed under the low strain rate conditions achieved with R = 0.1 and low frequency, as identified by the filled symbols in Fig. 12. This deviation was not observed at 50 °C when low strain rate conditions were achieved with higher R-ratio, nor was it observed in the studies performed at 21 °C [3]. The fatigue damage zones at two frequencies, 1 and 0.1 Hz, and the same loading conditions of R = 0.1 and $K_{I,mean}$ = 0.65 MPa $m^{1/2}$ are compared in Fig. 13. The zone obtained at the lower frequency was characterized by

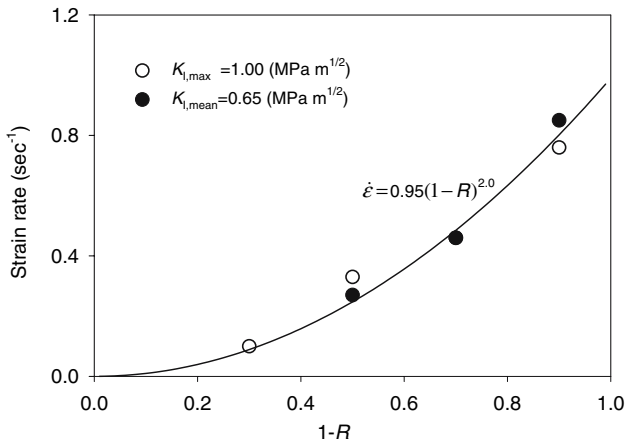

Fig. 11 The relationship between R-ratio and strain rate at the crack tip at 50 °C. The curve is the fit to $\dot{\varepsilon}=0.951(1-R)^{2.0}$

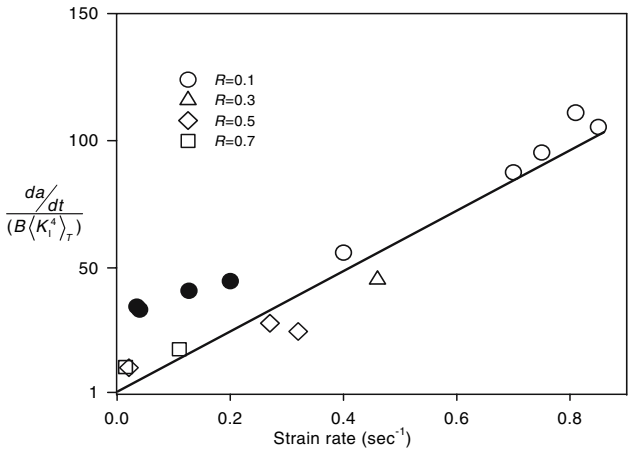

Fig. 12 Effect of strain rate on measured crack growth rate normalized to the calculated creep contribution to the crack growth rate at 50 °C. The filled symbols are tests at R = 0.1 and frequency 0.1 or 0.03 Hz

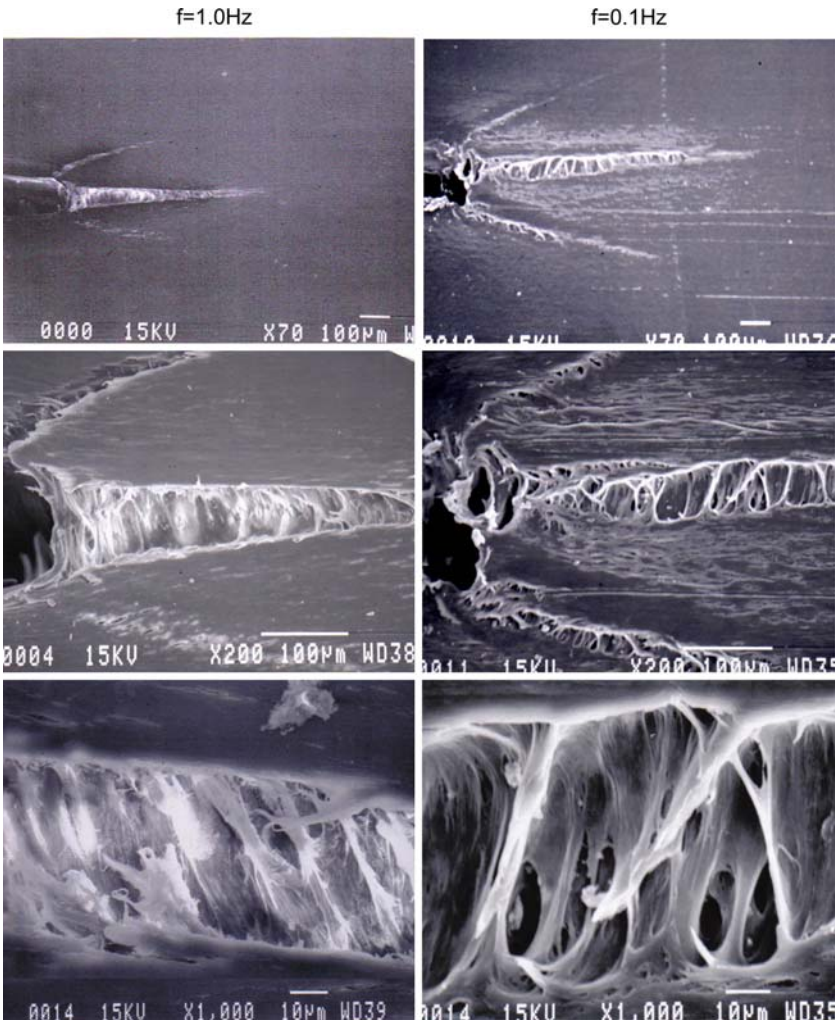

Fig. 13 SEM images of different magnification showing the entire crack tip craze zone, the crack tip region, and the craze fibrils for fatigue tests at frequency 1.0 Hz and frequency 0.1 Hz

a longer main craze, longer shear crazes and substantial damage in the region above and below the main craze.

Loading under $R = 0.1$ imposed the largest difference between $K_{I,max}$ and $K_{I,min}$, and also the lowest values of $K_{I,min}$. For example, at $K_{I.mean} = 0.65$ MPa $m^{1/2}$, $K_{I,min}$ was 0.12 MPa $m^{1/2}$ for $R = 0.1$ compared to 0.42 MPa $m^{1/2}$ for $R = 0.5$. In addition, the fibrils were much more extended at low frequency than at 1 Hz, as indicated by the high values of CTOD and ΔCTOD for specimens loaded at $f = 0.1$ and lower strain rate, Table 3. For example, the difference between maximum and minimum crack opening at $R = 0.1$ increased from 0.13 to 0.23 mm as frequency decreased from 1.0 to 0.03 Hz ($K_{I,mean} = 0.65$ MPa $m^{1/2}$).

It is speculated that under loading conditions of $R = 0.1$ and low strain rate, ΔCTOD exceeded the elastic recovery of the craze fibrils. As a result, the stretched fibrils were compressed and bent when the stored elastic energy closed the crack at $K_{I,min}$. The additional fibril damage reduced the craze lifetime to give the observed high crack speeds.

Conclusions

The present study was undertaken to determine whether the correlation between fatigue and creep established for polyethylene in air could be extended to environmental liquids. Stepwise fatigue crack growth in air was preserved in Igepal environmental liquids at 50 °C, the temperature specified for the ASTM standard. However, significant differences in the relationship between fatigue and creep were revealed by systematically decreasing the dynamic component of fatigue loading. In air, the lifetime steadily increased as the R-ratio (ratio of minimum to maximum load in the fatigue cycle) decreased to $R = 1$ (creep). In contrast, the lifetime in Igepal was affected to a much smaller extent. Under constant $K_{I,max}$ loading, the lifetime actually decreased as the R-ratio approached unity.

As a first step toward understanding the environmental effect, the stepwise mechanism of fatigue crack propagation at 50 °C in air was verified and the crack growth rate was related to the maximum stress and R-ratio by a power

law relationship. Alternatively, crack growth rate was modeled by considering a creep contribution that was calculated from the sinusoidal loading curve and the known dependence of creep crack growth rate on stress intensity factor, and a fatigue acceleration factor that depended only on strain rate. This study found that the strain rate approach, previously demonstrated for polyethylene resins at 21 °C, could be reliably used to correlate fatigue and creep at 50 °C under most loading conditions of stress, R-ratio and frequency. The exceptions were fatigue loading under conditions of $R = 0.1$ and frequency less than 1 Hz. It was speculated that fibril compression and bending were responsible for unexpectedly high crack speeds.

References

1. Parsons M, Stepanov EV, Hiltner A, Baer E (1999) J Mater Sci 34:3315, DOI: 10.1023/A:1004616728535
2. Parsons M, Stepanov EV, Hiltner A, Baer E (2000) J Mater Sci 35:1857, DOI: 10.1023/A:1004741713514
3. Parsons M, Stepanov EV, Hiltner A, Baer E (2000) J Mater Sci 35:2659, DOI: 10.1023/A: 1007354600584
4. Hu Y, Summers J, Hiltner A, Baer E (2003) J Mater Sci 38:633, DOI: 10.1023/A: 1021899801981
5. Bernal-Lara TE, Hu Y, Summers J, Hiltner A, Baer E (2004) J Mater Sci 39:2979, DOI: 10.1023/B: JMSC.0000025823.39995.40
6. Ward AL, Lu X, Huang Y, Brown N (1991) Polymer 32:2172
7. Qian R, Lu X, Brown N (1993) Polymer 34:4727
8. Tonyali K, Brown HR (1987) J Mater Sci 22:3287, DOI: 10.1007/BF01161193
9. Shanahan MER, Schultz J (1979) J Polym Sci: Polym Phys Ed 17:705
10. Hittmair P, Ullman R (1962) J Appl Polym Sci 19:1
11. Ward AL, Lu X, Brown N (1990) Polym Eng Sci 30:1175
12. Tonyali K, Rogers CE, Brown HR (1987) Polymer 28:1472
13. Mai YW, Williams JG (1979) J Mater Sci 14:1933, DOI: 10.1007/BF00551034
14. Altstaedt V, Keiter S, Renner M, Scharb A (2004) Macromol Symp 214:31
15. Parsons M, Stepanov EV, Hiltner A, Baer E (2001) J Mater Sci 36:5747, DOI: 10.1007/BF00705290
16. Chou CJ, Vijayan K, Kirby D, Hiltner A, Baer E (1988) J Mater Sci 23:2533, DOI: 10.1007/BF01111912
17. Shah A, Stepanov EV, Hiltner A, Baer E, Klein M (1997) Int J Frac 48:159
18. Shah A, Stepanov EV, Klein M, Hiltner A, Baer E (1998) J Mater Sci 33:3313, DOI: 10.1023/A: 1004360011750
19. Shah A, Stepanov EV, Capaccio G, Hiltner A, Baer E (1998) J Polym Sci: Part B: Polym Phys 36:2355
20. Brown N, Ward IM (1983) J Mater Sci 18:1405, DOI: 10.1007/BFO1111960
21. Lu X, Wang X, Brown N (1988) J Mater Sci 23:643, DOI: 10.1007/BF00576763
22. Berger LL, Kramer EJ (1987) Macromolecules 20:1980